Chemical Physics Letters 547 (2012) 47–51

Contents lists available at SciVerse ScienceDirect

Chemical Physics Letters

journal homepage: www.elsevier.com/locate/cplett

Single-molecule fluorescence of terrylene embedded in anthracene matrix: A room temperature study

M. Yavuz Yüce *, Alper Kiraz

Department of Physics, Koç University, Rumelifeneri Yolu, 34450 Sariyer, Istanbul, Turkey

ARTICLE INFO

Article history:
Received 6 June 2012
In final form 6 August 2012
Available online 11 August 2012

ABSTRACT

We characterized room-temperature fluorescence properties of single terrylene molecules embedded in anthracene thin films that were prepared by spin-coating on glass substrates. Our results show that terrylene molecules embedded in anthracene matrix are oriented nearly parallel to the substrate. Typical measured fluorescence lifetime of terrylene was 3.6 ns and photon count rate at saturation was 750 kHz. Our analyses of 104 molecules indicate that we can detect on average 1.6×10^6 photons from a single terrylene molecule before it photobleaches. These results make terrylene–anthracene a promising guest-host system for room temperature single molecule experiments.

1. Introduction

Over the last two decades single light emitters embedded in solid matrices have proven to be essential for numerous experimental realizations exploiting the quantum mechanical nature of light-matter interactions. In these demonstrations, different systems including semiconductor quantum dots, N–V centers in diamond, and dye molecules in crystalline hosts have been used [1,2]. Among these different systems, dye molecules embedded in crystalline hosts have proven to possess clear advantages due to the ease and cost of their experimental realization and highly coherent photons they emit at low temperatures [3]. They have been the system of choice for various quantum optical demonstrations including photon antibunching [4–6], two-photon interference [7–9], and guided emission [10,11].

Despite all the fascinating experimental results obtained with dye molecules over the last two decades, the number of dye-host matrix combinations having desirable optical and photophysical properties has not increased as fast. This makes any new dye-host combination valuable for extending the range of possible experiments [12–15]. A relatively recently introduced dye-host pair is the dibenzoterrylene (DBT)-anthracene system. Since the pioneering work in Ref. [13] this system has been successfully used in many other interesting demonstrations [8,10,16–19]. The DBT-anthracene system originated from the efforts to probe conduction in organic crystals using low-temperature single molecule spectroscopy. In fact, the first guest–host system explored for this goal was terrylene–anthracene [20,21]; however, the fluorescence intensity of terrylene turned out to be surprisingly low in these low temperature studies. This was attributed to a new type of intersystem crossing mechanism that also involved the host triplet state (intermolecular intersystem crossing), and occurred when the first excited electronic state of the dye was located at a higher energy level than the triplet state of the host molecule. This finding rendered DBT-anthracene to be a more favorable guest-host system compared to terrylene–anthracene. To our best knowledge, Refs. [20,21] are the only reports on characterizing terrylene fluorescence in anthracene matrix at the single molecule level, and a room temperature study of this system is still missing. In the present Letter, we aim to fill this gap by presenting our experimental results obtained with spin coated films of terrylene-doped anthracene.

Spin coating has been long known as a possible method for obtaining thin films of anthracene [22]. However its use in single molecule experiments to obtain thin films of dye-doped molecular crystals has been only recently demonstrated, by developing procedures for preparation of terrylene in *p*-terphenyl [23], and DBT in anthracene [19]. In comparison to the traditional sublimation method, the spin coating procedure used in Refs. [23,19] greatly facilitates sample preparation, reduces material costs, and allows preparation of much thinner films. In these Letters, authors have also reported a preferred orientation of the dye molecule within the host crystal, with dye molecule being perpendicular to the substrate for terrylene in *p*-terphenyl, and parallel to the substrate for DBT in anthracene. In our work, we also use spin coating to obtain terrylene-doped anthracene films, and characterize their optical properties at room temperature by performing single molecule studies.

This Letter is organized as follows. Following introduction, we continue with a description of sample preparation and experimental setup. Next, we present our results on characterization of the terrylene–anthracene system and quantify its performance. We finally summarize our results with concluding remarks.

* Corresponding author.
E-mail address: myuce@ku.edu.tr (M.Y. Yüce).

0009-2614/$ - see front matter © 2012 Elsevier B.V. All rights reserved.
http://dx.doi.org/10.1016/j.cplett.2012.08.014

2. Experimental

In order to obtain terrylene-doped anthracene films, we followed the procedure described in [19], except for using terrylene instead of DBT. The solution used for spin coating contained 2.6 mg/ml anthracene and ~100 nM terrylene dissolved in a 100/1 (by volume) mixture of diethyl ether/benzene. This was coated onto glass coverslips with a commercial spin coater (Specialty Coating Systems, P6700), at a speed of 3000 rpm for 30 s, followed by 1500 rpm for 20 s. Prior to coating, the coverslips were cleaned with a UV-Ozone cleaner (Jelight Company, 42-220) for 10 min.

Films prepared this way were then characterized using a home-built confocal microscope based on an inverted microscope frame (Nikon, Eclipse TE2000-U) with 1.49 NA oil immersion objective (Nikon, TIRF Apo 60x), and 90x total magnification. Samples were scanned using a piezoelectric scanning stage (Physik Instrumente; stage: P-733.3DD; controller: E-509.C3A) to obtain their fluorescence images, and locate individual molecules. Excitation was done at 532 nm with a tunable ultrafast laser system (Toptica, FFS; repetition rate: 80 MHz; linear polarization, pulsewidth < 1 ps) and a suitable dichroic mirror (Chroma, z532/1064rpc). All the values of excitation power, P, mentioned in the text were measured at the objective nosepiece of the microscope with a wide-area detector (Thorlabs, S120B). Excitation intensities at the focal point (averaged over the region $0 < r < \omega_0$, where ω_0 is the $1/e^2$ radius) were calculated from power measurements assuming a Gaussian intensity profile. A half waveplate (Thorlabs, WPMH05M-532) mounted on a custom-made motorized holder was used to rotate the polarization of the excitation beam, when necessary. Similarly, a polarizer (Melles Griot PSP-450-750-10) mounted on a more precise but slower rotation stage (Standa) was used for polarization dependent analysis of terrylene fluorescence emission.

Light collected from the sample was sent either to a pair of avalanche photodiode detectors (APD; Perkin Elmer, SPCM-AQR-13; dark counts: 250 cps), or to a monochromator (Princeton Instruments, SP2750; focal length: 750 mm, grating: 300 grooves/mm) equipped with a thermoelectrically-cooled spectroscopic camera (Princeton Instruments, PIXIS eXcelon-100B). For detection with APDs, light from the sample was first focused onto a pinhole (Thorlabs, P50S; diameter: 50 μm) with the microscope's tube lens, thus rejecting the out-of-focus light. Subsequently, spatially filtered beam was collimated, passed through appropriate notch (Chroma, ZET532NF) and bandpass (Chroma, HQ605/90M) filters, split into two parts with a 50/50 beamsplitter (Thorlabs, BSW10), and finally focused onto the APDs. A short-pass filter (Thorlabs, FES0700) was placed between the two APDs to prevent any infrared photons generated on one APD from being detected by the other. The pulses from the APDs were fed either to the start and stop channels of a time-to-amplitude converter (TAC; Ortec, 566), or to the counters of a multi-purpose data acquisition card (National Instruments, PCIe-6363). By employing asynchronous detection with the card, we measured photon arrival times with 10 ns resolution, and subsequently calculated the cross-correlation of the intensities detected by two APDs using a fast algorithm [24]. In order to record the terrylene spectra, a long-pass filter (Thorlabs, FEL0550) was placed at the entrance of the monochromator to reject the red tail of the pump laser that overlapped with the spectral window of interest in our measurements.

3. Results and discussion

A representative confocal fluorescence image of terrylene molecules in anthracene film is shown in Figure 1. The image is 4 × 4 μm in size, consists of 100 × 100 pixels, and was acquired with 1 ms/pixel integration time under an excitation intensity of 12 kW/cm^2 (P = 10 μW). The bright features in this image are candidate locations for individual terrylene molecules. Being ~1 nm in size, a terrylene molecule acts as a point source, and its image reveals the diffraction-limited waist of the excitation beam at the focal plane. The intensity profile along a line drawn across one of the features shown in Figure 1 (marked by A and B) is plotted in the inset. A Gaussian function fitted to this profile gives a FWHM of 223 nm, in agreement with our expectation for a confocal single molecule image at the given excitation wavelength. The varying intensity of the features is attributed to different orientations of terrylene molecules within the host crystalline matrix. In general, molecules with their transition dipole moments oriented parallel to the (linear) excitation beam polarization vector are excited more efficiently.

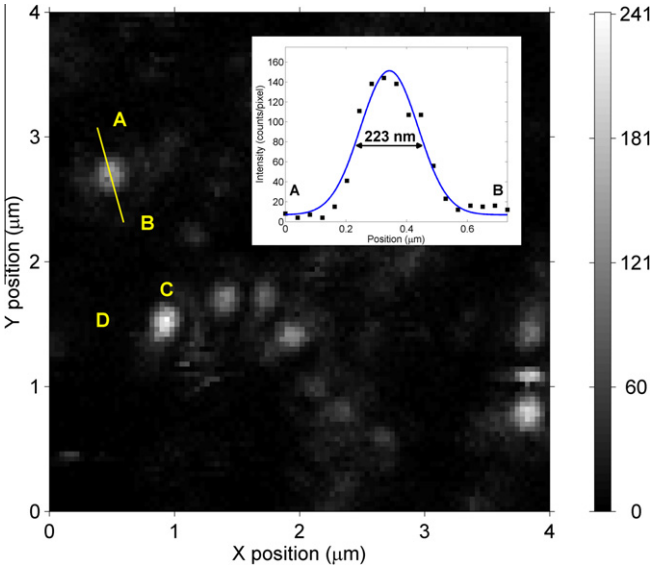

Figure 1. Confocal image of individual terrylene molecules in anthracene, recorded from a 4 μm × 4 μm area with 100 × 100 pixels, and 1 ms/pixel integration time. Excitation intensity was 12 kW/cm^2 (P = 10 μW). Inset shows the intensity profile (black squares) taken along the center of the upper left molecule, and a Gaussian fit (blue line) to it. Width of the Gaussian function is 223 nm, in agreement with the diffraction limited resolution. The colorbar designates the number of photons detected per pixel. (For interpretation of the references to color in this figure legend, the reader is referred to the web version of this article.)

In order to verify that the bright features in Figure 1 indeed correspond to individual terrylene molecules, we positioned one of them (marked by C) within the excitation focal spot, and recorded its fluorescence spectrum (Figure 2a) and a TAC histogram (Figure 2b) from it. Both data sets were recorded for 1 min, using the same excitation intensity as the one used during scanning. The background correction for the spectrum was done by recording a second spectrum at an empty position within the sample (marked by D) with identical conditions (i.e. with the excitation laser on), and subtracting this from the molecule spectrum recorded at point C. The resulting fluorescence spectrum given in Figure 2a shows a peak emission wavelength of 579.3 nm and a second peak at around 630 nm, in agreement with the characteristic spectrum of terrylene in a similar crystalline host [25]. On the other hand, photon antibunching effect represented by a missing peak at the zero delay time of the TAC histogram in Figure 2b is characteristic for a single emitter. Noting that these two data sets were collected from the same position, we can conclude that the bright features in the confocal image of Figure 1 truly correspond to single terrylene molecules.

To calculate the fluorescence lifetime of terrylene in anthracene matrix, we fitted the data of Figure 2b with the following model

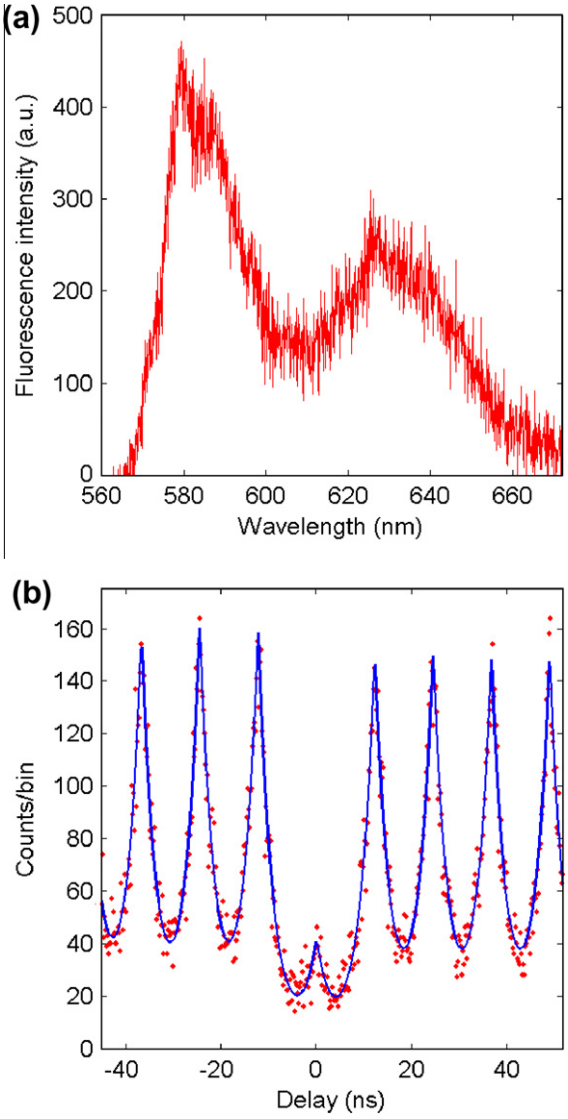

Figure 2. (a) Fluorescence spectrum recorded from one of the bright features (marked by C) in the confocal image of Figure 1. (b) TAC histogram (red diamonds) recorded from the same position, and fitted with the exponential model described in the text (blue line). TAC rate was 537 Hz. (For interpretation of the references to color in this figure legend, the reader is referred to the web version of this article.)

$$C(\tau) = \sum_n A_n e^{\frac{|\tau - nT|}{\tau_F}}, \quad (1)$$

where $C(\tau)$ is the coincidence count, τ is the TAC delay time, τ_F is the fluorescence lifetime, T is the time between consecutive laser pulses, and n and A_n are the order and weight of the peaks corresponding to individual excitation pulses [1]. Using this model, we obtained $\tau_F = 3.0$ ns for the molecule of Figure 2b. The same analysis made over 41 individual molecules resulted in an average fluorescence lifetime of $\tau_F = 3.6 \pm 0.5$ ns, which is in good agreement with the value of 3.15 ± 0.1 ns reported in [20,21], and significantly shorter than fluorescence lifetimes observed with other hosts [26].

In order to gain insight about the orientation of terrylene molecules in our spin coated anthracene films, we mounted a polarizer into the detection path, and observed the fluorescence intensity of a single molecule as the polarizer was rotated. This measurement configuration can be considered as a one-dimensional version of the polarization-portraying technique proposed recently for studying energy transfer or conformational properties of multichromophoric systems [27]. As shown in Figure 3, the fluorescence intensity exhibited a clear cosine-square dependency on the polarizer angle (trace A). High modulation depth indicates that the terrylene molecules are oriented such that their transition dipole moments are nearly parallel to the plane defined by the anthracene film (i.e. perpendicular to the optical axis). Similar in-plane orientation has been observed also for single DBT molecules in anthracene [19], and shown to be a desired property in a microcavity design [10]. Next, we carried out the same measurement at an empty position within the host crystal, 0.8 μm away from the molecule (trace B). This provided us the background level present in the previously acquired single molecule data. The background count rates in trace B remained lower than the dip of the modulated single molecule fluorescence in trace A, suggesting that the transition dipole moment was not located perfectly in the plane of the anthracene film. It should be noted that the same observation (i.e. dip of trace A remaining above trace B) can also be interpreted as an ellipticity in fluorescence polarization introduced by oblique elements in the detection path such as beamsplitter or port selection prism [28]. Nevertheless even in the presence of an artifact, one can still ignore any depolarization and attempt to quantify the out-of-plane component as if the not-prefect modulation were completely due to dipole orientation. The result in this case will be an upper bound for the angle between a terrylene molecule and the film plane. To do this analysis, we followed a method proposed in Ref. [29]. We first used the background-subtracted count rates (trace B subtracted from trace A) to determine the fluorescence intensities corresponding to cases when the polarizer axis is parallel, at 45°, and orthogonal to the transition dipole moment as 160, 97, and 24 kHz, respectively. Then, using these count rates in equations 5–8 of [29], we calculated that the transition dipole moment is out of plane by at most 28°. The same analysis carried over 21 single molecules and respective background data resulted in an average value of 35 ± 11°.

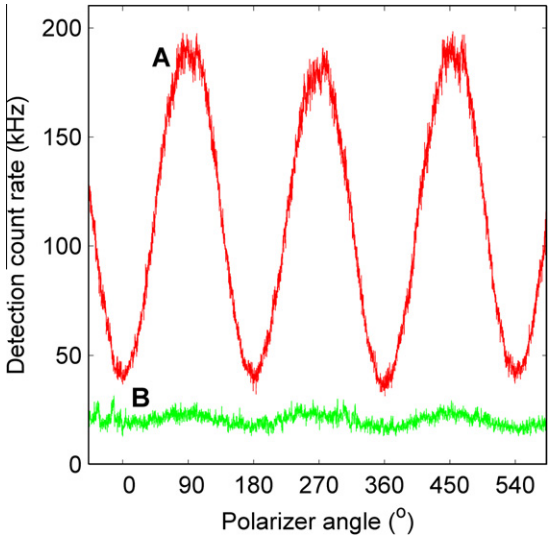

Figure 3. Change in detection rates, as the emission from a single Terrylene molecule (trace A; red) and an empty position within the anthracene crystal (trace B; green) are passed through a rotating polarizer mounted between the microscope and the detectors. Excitation light was linearly polarized with fixed direction. The high modulation depth in trace A is an indicative of the parallel orientation of the molecule's transition dipole moment with respect to the substrate plane. Excitation intensity was 68 kW/cm^2 ($P = 55$ μW) for both measurements. Integration time of the original intensity versus time data was 10 ms. (For interpretation of the references to color in this figure legend, the reader is referred to the web version of this article.)

As a next step for characterizing the terrylene-anthracene system, we recorded fluorescence saturation curves from single mol-

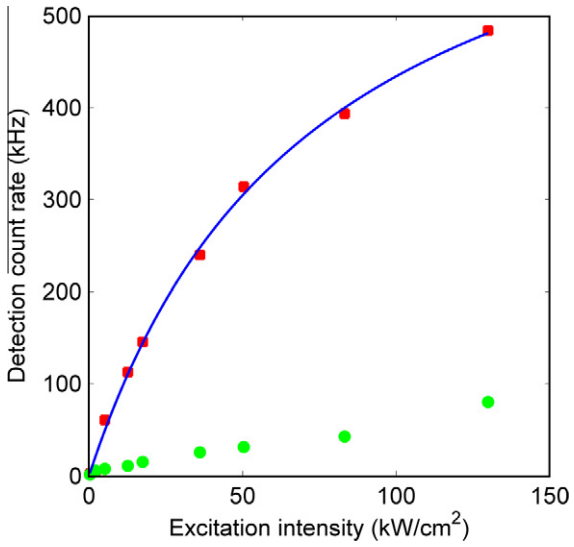

Figure 4. Detection rates for the fluorescence of a single terrylene molecule (red squares) and the background (green circles) plotted as a function of the excitation intensity. The fluorescence signal is fitted with a standard saturation model to yield a detection rate at saturation of S_∞ = 750 kHz (blue line). (For interpretation of the references to color in this figure legend, the reader is referred to the web version of this article.)

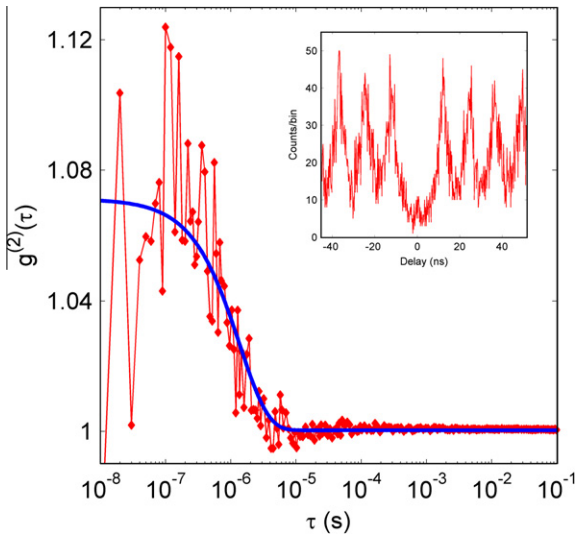

Figure 5. Intensity autocorrelation function of a single terrylene molecule (red diamonds), fitted with an exponential decay (blue line). Excitation intensity was 12 kW/cm^2 (P = 10 μW), corresponding to a total count rate of 137 kHz on the APD's. A TAC histogram recorded from the same molecule is shown in the inset. (For interpretation of the references to color in this figure legend, the reader is referred to the web version of this article.)

ecules. Figure 4 shows one such curve, where the background-subtracted signal (red squares), and the background (green circles) are plotted as a function of the excitation intensity. The background rates were recorded following photobleaching from the position of a specific molecule. We fitted the fluorescence rates using the well-known saturation model

$$S(P) = S_\infty \frac{I/I_{sat}}{1 + I/I_{sat}} \tag{2}$$

where S is the fluorescence detection rate, I is the excitation intensity, I_{sat} is the saturation intensity, and S_∞ is the fluorescence detection rate at saturation [16]. The fit yielded I_{sat} = 74 kW/cm^2 (P_{sat} = 60 μW), and S_∞ = 750 kHz, which were moderate values considering several other terrylene molecules we analyzed.

It is interesting to note that the typical S_∞ value obtained at room temperature is orders of magnitude larger than the one reported in previous studies at cryogenic temperatures (≈750 kHz versus ≈300 Hz) [20,21]. Although the oil immersion objective we used in our experiments brings a clear advantage over a simple aspheric lens used in [20,21], the discrepancy is still too large to be attributed to the numerical aperture of the lenses alone. A plausible explanation could be in the orientation of terrylene molecules within the host crystal, which has a significant influence on the collection efficiency. However, the possibility of an unfavorable orientation was already addressed in Ref. [21], and ruled out based on control experiments with another host, naphthalene. In addition to this conclusion, we point out the similarity between sublimation-grown [21] and spin-cast [22] anthracene films, both of which were reported to extend along the (a,b) plane. A similar morphology has also been observed for crystals obtained from solution [30] and vapor phase [31], indicating that we should not expect a dramatic change in molecular organization within anthracene films prepared by different methods. Consequently, the anthracene morphology that favored in-plane orientation of terrylene molecules in our samples was most probably also present in Refs. [20,21]. Another reason for the low fluorescence signal in these studies could be the position of the dye molecule with respect to the aspheric lens or the interfaces, which is mainly determined by the thickness of the host film. Regarding this possibility we note that the same host crystal was used in Ref. [13] with the same sample preparation steps, to obtain DBT-doped anthracene films. The resulting fluorescence signal in this case was sufficient. Had there been problems originating from molecules' position or film thickness in Ref. [20,21], these would also appear in the DBT-anthracene system. In our opinion, the above comparison leaves temperature as the only differing parameter that can explain the two contrasting S_∞ values. Therefore we conjecture that the intermolecular intersystem crossing mechanism proposed in references [20,21] may be a temperature dependent phenomenon.

Following Ref. [21], we also performed correlation analysis to calculate the intersystem crossing yield at room temperature. Figure 5 shows the autocorrelation function, $g^{(2)}(\tau)$, calculated from intensity versus time data of a single terrylene molecule with I = 12 kW/cm^2 excitation intensity (P = 10 μW) and 30 s acquisition time (red diamonds). The autocorrelation function was fitted with a mono-exponential model $g^{(2)}(\tau) = 1 + Ce^{-\lambda\tau}$, yielding a contrast of C = 0.071, and a decay parameter of $\lambda = 7 \times 10^5$ Hz (blue line). The population and depopulation rates of the triplet state, denoted by k_{23} and k_{31}, respectively, were then calculated from the fit parameters using relations

$$C = \frac{\lambda - k_{31}}{k_{31}} \tag{3}$$

and

$$\lambda = k_{31}\left[1 + \frac{I/I_{sat}}{1 + (2k_{31}/k_{23})(1 + I/I_{sat})}\right] \tag{4}$$

where I_{sat} was taken as 74 kW/cm^2 based on the analysis of Figure 4. The obtained k_{23} and k_{31} rates are 1×10^6 and 7×10^5 Hz, respectively. In comparison to the values reported at cryogenic temperatures in [21] ($k_{23} = 1.0 \pm 0.5 \times 10^6$ Hz, $k_{31} = 1.8 \pm 0.3 \times 10^3$ Hz), we can see that the triplet state is populated with almost the same rate, whereas the depopulation rate k_{31} is much faster for our case. Noting the strong relation between k_{31} and λ, we wanted to confirm that the observed decay in the autocorrelation function was not an artifact due to other effects such as laser intensity fluctuations. For this, we calculated the autocorrelation function of a laser beam reflected from an empty coverslip, and observed that it was distrib-

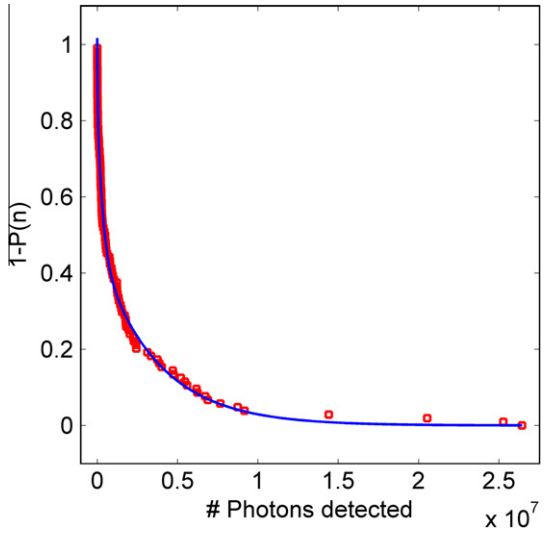

Figure 6. Probability distribution of the number of photons detected before photobleaching, obtained from a set of 104 single molecule measurements (red squares), and fitted with a tri-exponential decay function (blue line). Excitation intensity was 24 kW/cm^2 (P = 19 μW). (For interpretation of the references to color in this figure legend, the reader is referred to the web version of this article.)

uted symmetrically around $g^{(2)}(\tau) = 1$, as expected (data not shown). A TAC histogram recorded from the same molecule is presented in the inset; using this histogram, we fitted the fluorescence lifetime as $\tau_F = (k_{21} + k_{23})^{-1} = 3.6$ ns, using the same model as in Figure 2b. The intersystem crossing yield was then calculated as $k_{23}/(k_{21} + k_{23}) = 4 \times 10^{-3}$, which is comparable to its reported low-temperature value of $(3 \pm 2) \times 10^{-3}$ [21].

Finally, we addressed the issue of photostability of the terrylene–anthracene system through statistical analysis of intensity-versus-time data recorded from individual molecules as suggested by [32,33]. Since the survival time of a molecule depends on the excitation intensity, and blinking events impose difficulties in quantifying it, we used the number of photons detected before bleaching as our measure of photostability. To ensure equal excitation efficiency for all azimuthal orientations of the molecular transition dipoles, we mounted a half-waveplate into the excitation path, and rotated it at an angular frequency of ≈1.7 Hz. This resulted in a temporally modulated fluorescence signal, which provided an extra indication of single molecule observation in addition to one-step photobleaching. Figure 6 shows the probability distribution of the number of photons detected before bleaching, obtained from a set of 104 molecules (red squares). The distribution could not be fitted by mono- or bi-exponential decays, indicating some degree of heterogeneity within the studied molecular population. A tri-exponential fit yielded the characteristic numbers of detected photons as 1×10^4, 3.3×10^5 and 3.6×10^6, with weights 0.19, 0.37 and 0.44, respectively. It is not clear to us if this heterogeneity is inherent to the terrylene–anthracene system, or related to sample preparation. The weighted average for the characteristic number of detected photons is 1.6×10^6, which is sufficient for most of the single molecule experiments.

4. Conclusion

We evaluated the potential of terrylene-doped anthracene thin films for use in single molecule experiments at room temperature. The short fluorescence lifetime, mostly in-plane orientation of the dye molecules within the host matrix, high detection rate at saturation, fast triplet state depopulation rate, and fair photostability all make this system a good candidate for room temperature studies. We expect that our results will also be beneficial for further studies aimed at understanding the intermolecular intersystem crossing mechanism in this guest–host system.

Acknowledgements

This work was partially supported by T.R. Ministry of Development under Grant No. 2009K120200. M.Y.Y. acknowledges TUBITAK for Ph.D. scholarship (BIDEB-2211).

References

[1] B. Lounis, M. Orrit, Rep. Prog. Phys. 68 (2005) 1129.
[2] A.J. Shields, Nat. Photon. 1 (2007) 215.
[3] A. Kiraz, M. Ehrl, C. Bräuchle, A. Zumbusch, Appl. Phys. Lett. 85 (2004) 920.
[4] Th. Basché, W.E. Moerner, M. Orrit, H. Talon, Phys. Rev. Lett. 69 (1992) 1516.
[5] L. Fleury, J.-M. Segura, G. Zumofen, B. Hecht, U.P. Wild, Phys. Rev. Lett. 84 (2000) 1148.
[6] F. Treussart, A. Clouqueur, C. Grossman, J.-F. Roch, Opt. Lett. 26 (2001) 1504.
[7] A. Kiraz, M. Ehrl, Th. Hellerer, Ö.E. Müstecaplıoğlu, C. Bräuchle, A. Zumbusch, Phys. Rev. Lett. 94 (2005) 223602.
[8] J.B. Trebbia, P. Tamarat, B. Lounis, Phys. Rev. A 82 (2010) 063803.
[9] R. Lettow, Y.L.A. Rezus, A. Renn, G. Zumofen, E. Ikonen, S. Götzinger, V. Sandoghdar, Phys. Rev. Lett. 104 (2010) 123605.
[10] C. Toninelli, Y. Delley, T. Stöferle, A. Renn, S. Götzinger, V. Sandoghdar, Appl. Phys. Lett. 97 (2010) 021107.
[11] K.G. Lee et al., Nat. Photon. 5 (2011) 166.
[12] S. Kummer, Th. Basché, C. Bräuchle, Chem. Phys. Lett. 229 (1994) 309.
[13] C. Hofmann, A. Nicolet, M.A. Kol'chenko, M. Orrit, Chem. Phys. 318 (2005) 1.
[14] M. Pärs, V. Palm, M. Rähn, N. Palm, J. Kikas, J. Lumin. 128 (2008) 838.
[15] A.A. Gorshelev, A.V. Naumov, I.Yu. Eremchev, Y.G. Vainer, L. Kador, J. Köhler, ChemPhysChem. 11 (2010) 182.
[16] A.A.L. Nicolet, C. Hofmann, M.A. Kol'chenko, B. Kozankiewicz, M. Orrit, ChemPhysChem. 8 (2007) 1215.
[17] A.A.L. Nicolet, P. Bordat, C. Hofmann, M.A. Kol'chenko, B. Kozankiewicz, R. Brown, M. Orrit, ChemPhysChem. 8 (2007) 1929.
[18] J.B. Trebbia, H. Ruf, Ph. Tamarat, B. Lounis, Opt. Express 17 (2009) 23986.
[19] C. Toninelli, K. Early, J. Bremi, A. Renn, S. Götzinger, V. Sandoghdar, Opt. Express 18 (2010) 6577.
[20] M.A. Kol'chenko, B. Kozankiewicz, A. Nicolet, M. Orrit, Opt. Spectrosc. 98 (2005) 681.
[21] A. Nicolet, M.A. Kol'chenko, B. Kozankiewicz, M. Orrit, J. Chem. Phys. 124 (2006) 164711.
[22] E. ten Grotenhuis, J.C. van Miltenburg, J.P. vander Eerden, Chem. Phys. Lett. 261 (1996) 558.
[23] R.J. Pfab, J. Zimmermann, C. Hettich, I. Gerhardt, A. Renn, V. Sandoghdar, Chem. Phys. Lett. 387 (2004) 490.
[24] M. Wahl, I. Gregor, M. Patting, J. Enderlein, Opt. Lett. 11 (2003) 3583.
[25] F. Kulzer, F. Koberling, Th. Christ, A. Mews, Th. Basché, Chem. Phys. 247 (1999) 23.
[26] G.S. Harms, T. Irngartinger, D. Reiss, A. Renn, U.P. Wild, Chem. Phys. Lett. 313 (1999) 533.
[27] O. Mirzov, R. Bloem, P.R. Hania, D. Thomsson, H. Lin, I.G. Scheblykin, Small 5 (2009) 1877.
[28] R. Camacho, D. Thomsson, D. Yadav, I.G. Scheblykin, Chem. Phys., 2012, doi:10.1016/j.chemphys.2012.03.001.
[29] J.T. Fourkas, Opt. Lett. 26 (2001) 211.
[30] P. Zhang et al., J. Cryst. Growth 311 (2009) 4708.
[31] S. Jo, H. Yoshikawa, A. Fujii, M. Takenaga, Appl. Surf. Sci. 252 (2006) 3514.
[32] A. Molski, J. Chem. Phys. 114 (2001) 1142.
[33] C. Jung, B.K. Müller, D.C. Lamb, F. Nolde, K. Müllen, C. Bräuchle, J. Am. Chem. Soc. 128 (2006) 5283.